First-principles molecular-dynamics study of the (0001) α-quartz surface

G.-M. Rignanese

Unité de Physico-Chimie et de Physique des Matériaux, Université Catholique de Louvain, 1 Place Croix du Sud,
B-1348 Louvain-la-Neuve, Belgium
and Institut Romand de Recherche Numérique en Physique des Matériaux (IRRMA), Ecublens, CH-1015 Lausanne, Switzerland

Alessandro De Vita

Institut Romand de Recherche Numérique en Physique des Matériaux (IRRMA), Ecublens, CH-1015 Lausanne, Switzerland
and INFM and Dipartimento di Ingegneria dei Materiali, Università di Trieste, via A. Valerio 2, 34127 Trieste, Italy

J.-C. Charlier

Unité de Physico-Chimie et de Physique des Matériaux, Université Catholique de Louvain, 1 Place Croix du Sus,
B-1348 Louvain-la-Neuve, Belgium
and Institut Romand de Recherche Numérique en Physique des Matériaux (IRRMA), Ecublens, CH-1015 Lausanne, Switzerland

X. Gonze

Unité de Physico-Chimie et de Physique des Matériaux, Université Catholique de Louvain, 1 Place Croix du Sud,
B-1348 Louvain-la-Neuve, Belgium

Roberto Car*

Institut Romand de Recherche Numérique en Physique des Matériaux (IRRMA), Ecublens, CH-1015 Lausanne, Switzerland
and Department of Condensed Matter Physics, University of Geneva, CH-1211 Geneva, Switzerland

(Received 4 October 1999)

We present an *ab initio* investigation of the structural and electronic properties of the (0001) α-quartz surface. Five different models of this surface are generated by cleavage of the bulk followed by atomic relaxation and constant-temperature molecular dynamics. The most favorable reconstruction presents an unexpected densification of the two uppermost layers of SiO_2 tetrahedral units, with three-membered and six-membered rings that do not exist in bulk α-quartz. The electronic density of states for this surface is very similar to the bulk one, except for a typical feature of SiO_2 under pressure, namely the disappearance of the gap between Si-O bonding and O $2p$ nonbonding states.

I. INTRODUCTION

SiO_2 plays an important role in many advanced technological fields. It can be used as a substrate for silicon in microelectronics,[1] for oxide multilayers in optics, for metallic multilayers in magnetics, or for polymers in the field of adhesion.[2] In all these cases, the interface properties are expected to be strongly dependent on the initial SiO_2 surface atomic structure. Amongst the various surfaces of the different crystallographic forms of SiO_2, the (0001) α-quartz surface can be considered as a model surface due to important common characteristics such as the SiO_4 tetrahedral building blocks and Si or O coordination numbers. Furthermore, the study of this crystalline surface may also be useful to better understand amorphous silica surfaces.

Whereas the bulk quartz structure has been widely studied, the experimental data on the structure of quartz surfaces are rather scarce. To our knowledge, there have been only two experimental determinations of the crystallographic structure of the (0001) α-quartz surface. A slight chemical etching in HF leads to the appearance of a 1×1 pattern;[3] a $\sqrt{84} \times \sqrt{84}$ reconstruction with a rotation angle of 11° is observed for temperatures greater than 600° C.[4] The experimental study of insulating surfaces is more difficult than that of conducting surfaces, since most standard surface analysis techniques involve charged particles (ions, electrons), in incident beams or as outgoing particles. Some progress has been recently made in this field. For instance, the quartz surface has been studied using atomic force microscopy (AFM), providing information on its microscopic structure.[5] However, the low contrast of the AFM pictures at the atomic scale still precluded crystallographic structure determination.

In most experimental techniques, data are collected over a very long time in comparison with atomic motion, and the direct observation of a particular event or structure is thus not allowed. By contrast, molecular-dynamics (MD) simulations permit a detailed analysis of atomic motion and of complex microstructures. Using this technique, much progress has been achieved in the study of vitreous silica surfaces. These simulations were invariably based on semiempirical potentials.[6–9]

In this paper, we present a *first-principles* molecular-dynamics investigation of the (0001) α-quartz surface. We determine various atomic structures which could appear upon fracture of bulk material. In principle, the selection of the final structure depends on the thermal and chemical (atmospheric) exposure of the surface atoms, and not just on the motion of surface atoms upon the fracture. For simplicity, we

deal with surfaces obtained in a perfect vacuum (i.e., in absence of water), thus focusing on the second effect only. The fracture of bulk quartz perpendicularly to the (0001) direction could produce two fundamental types of surfaces: terminating either with Si atoms, or with an oxygen atom attached to each silicon atom of the Si-terminated case. Since natural silicon dioxide surfaces are generally assumed to terminate with hydroxyl (OH) groups,[10,11] the oxygen-terminated surface is probably more representative of real conditions. Electrostatic and stoichiometry arguments support this choice, so that we concentrate on this type of surface. We consider two initial configurations: the cleaved surface with nonbridging oxygens at the top and a 2×1 reconstruction with edge-sharing tetrahedra. We then derive two reconstructions from atomic relaxation of the 2×1 reconstruction. We finally obtain two more reconstructions by constant-temperature first-principles MD simulations. The first of these two last structures, from here on named valence alternation pair (VAP) surface, presents an intimate pair of over- and undercoordinated oxygen atoms near the surface with three-membered rings. The second, which we call dense surface, presents a densification of the two uppermost layers of SiO_2 tetrahedral units, with three-membered and six-membered rings, in which each O atom is connected to two Si atoms, while each Si atom is connected to four O atoms, as in the bulk. This feature only appears in this model. We compute the surface energies of these structures, and find that the dense surface is the most stable one. Its calculated electronic density of states is very similar to that of bulk α-quartz. However, as for SiO_2 under pressure,[12,13] the gap between Si-O bonding and O $2p$ nonbonding states vanishes, indicating a strong hybridization between these states.

II. COMPUTATIONAL DETAILS

In all our calculations, the atomic positions are fully relaxed using the Car-Parrinello method[14,15] within the local density approximation (LDA) to density-functional theory,[16] which provides the electronic structure as well as the forces that act on the ions. The choice of the LDA is motivated by the following facts. On one hand, the LDA has proven to reproduce very accurately the structural properties of α-quartz.[17] On the other hand, although the generalized gradient approximation (GGA) was recently reported to correct a qualitative error of the LDA in the energy difference between two polymorphs of SiO_2, it does not improve over the structural properties with respect to LDA (errors in the lattice parameters and bond length are in the 1–2 % range for both LDA and GGA).[18] In this study, all the structures considered are not too far from the ideal quartz. Hence, we will restrict ourselves to the use of the LDA. A subsequent study using the GGA (Ref. 19) has shown that the energy ordering of the various structures considered hereafter is not changed, even though the energy differences are slightly different.

In our simulations, only valence electrons are explicitly considered. We use norm conserving pseudopotentials[20] to model the core-valence interaction. The electronic wave functions are expanded into plane waves up to a kinetic energy cutoff of 50 rydbergs. Exchange and correlation effects are calculated using Perdew and Zunger's interpolation formulas.[21] The Brillouin zone (BZ) sampling is limited to the Γ point only.

A preliminary simulation of bulk quartz is performed to serve as a reference for the absolute surface energy calculations and to determine the initial bond lengths and angles to be used in the actual surface simulations. For this purpose, we use a tetragonal unit cell of sides $a = 9.62$ Å, $b = 8.34$ Å, and $c = 10.64$ Å derived from the theoretical equilibrium lattice constant.[22] This periodic cell contains 24 Si atoms and 48 O atoms [corresponding to 6 O-Si-O layers along the (0001) direction]. The calculated Si-O bond length in bulk quartz is 1.605 ± 0.005 Å, differing less than 1 % with the experimental value.[23] The Si-O-Si angle distribution is peaked around 139° (experimental value: 143.73°), whereas the four values of O-Si-O angles are 108.1°, 109.3°, 109.4°, and 111.0°, respectively (experimental values: 108.81°, 108.93°, 109.24°, and 110.52°). All these values present less than 5 % discrepancy with experimental data.[23]

In our surface simulations, we consider a periodic tetragonal cell containing a SiO_2 slab and a vacuum region. The procedure to generate the slab, by repeating O-Si-O layers along the (0001) direction, meets the requirement of charge neutrality in the cell and avoids large dipole moments. The initial bond lengths and angles in the O-Si-O layers are taken from the preliminary simulation of bulk quartz. The periodic cell has a surface unit of sides $a = 9.62$ Å and $b = 8.34$ Å, derived from the theoretical equilibrium lattice constant of α-quartz.[22] In the direction orthogonal to the surface, the cell contains six monolayers of SiO_2 (9.5 Å), the bottom extremities being saturated with hydrogen atoms, for a total (slab + vacuum) length of $c = 15.88$ Å. Hence, our systems contain 24 Si atoms, 44 O atoms, and 8 H atoms. In the minimization process, the atoms of the lowest SiO_2 monolayer are kept fixed. After the atomic relaxation, the stability of each configuration is studied by performing constant-temperature molecular-dynamics simulations.[24]

Finally, in order to obtain absolute surface energies, we use a different geometry for the surface models, namely, we consider a symmetric slab (hence including two surfaces). In this case, the dimension of the tetragonal cell in the direction orthogonal to the surface is $c = 26.46$ Å (slab + vacuum), containing $n = 10$ or 12 monolayers of SiO_2, and the atoms of the two central SiO_2 monolayers are kept fixed during the atomic relaxation process. The absolute surface energy E_{surf} is the difference between the total energy of the slabs of increasing thickness $E_{slab}(n)$ (where n is the number of O-Si-O layers) and those of bulk systems containing the same number of atoms:

$$E_{surf} = \frac{1}{2} \left(E_{slab}(n) - n \frac{E_{bulk}}{6} \right),$$

where E_{bulk} is the total energy of the reference bulk system described above (which contains $n = 6$ O-Si-O layers).

III. SURFACE MODELS AND DISCUSSION

We first describe the most important structural features of our models. A detailed analysis, that can be found elsewhere,[25] shows that within 5 Å from the surface, the bulk
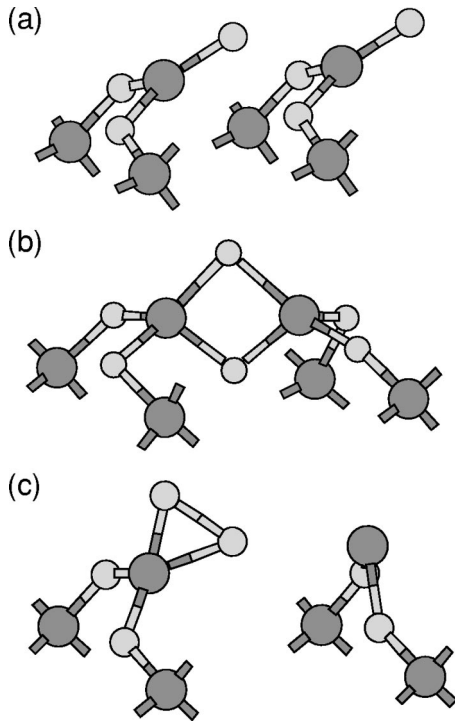
FIG. 1. Side view of (a) the cleaved surface, (b) an hypothetical 2×1 reconstruction with edge-sharing tetrahedra, and (c) the dimer surface. Si and O atoms are represented in dark and pale gray, respectively.

structure is recovered and that only limited strain occurs in the O-Si-O layers just above the fixed one. Thus, the size of the SiO$_2$ slab used in the simulations is large enough to simulate an ideal semi-infinite solid.

A. The cleaved surface and the dimer surface

The simplest model for the α-quartz (0001) surface is obtained simply by interrupting the repetition of the O-Si-O layers. We will refer to it as the *cleaved surface*. This 1×1 geometry of the surface is characterized by one non-bridging oxygen and one three-coordinated silicon per surface unit cell [Fig. 1(a)].

The second and third models for the α-quartz are constructed starting from the idea that the structure would be more stable if a connected tetrahedral framework were recovered at the surface. This corresponds to replacing non-bridging oxygens and three-coordinated silicons by two-coordinated oxygens and four-coordinated silicons, respectively.

We can easily do this by considering a 2×1 reconstruction in which originally nonbridging oxygens connected to two surface silicons (three-coordinated in the cleaved surface) form edge-sharing tetrahedra (two-membered rings), as shown in Fig. 1(b).

However, a simple atomic relaxation of this surface leads to a completely different structure [Fig. 1(c)]. The two oxygens that should be shared by two silicons prefer to form an O$_2$ dimer on one of the latter, leaving the other silicon only twofold coordinated. This structure, which we refer to as the *dimer surface*, is energetically unfavorable with respect to the cleaved surface (cf. Table I).

TABLE I. Computed surface energies for the five different models: dimer, cleaved, VAP, semidense, and dense surfaces in ascending order of stability (the type of reconstruction is given in parentheses). The surface energies are expressed in eV/Å^2. The number of Si-O bonds per Si atom (# Si-O) has also been indicated for the two Si atoms in the first layer of a 2×1 surface unit-cell.

Model	Energy	# Si-O
Dimer (2×1)	0.25	2,4
Cleaved (1×1)	0.17	3,3
VAP (2×1)	0.14	4,4
Semidense (2×1)	0.09	4,4
Dense (1×1)	0.05	4,4

A contour plot of electronic density on the dimer is represented in Fig. 2. The dimerization of the two oxygens clearly appears from the picture (the O-O distance is 1.60 Å), which also shows an increased electronic density at the two-fold coordinated silicon with respect to the other four-coordinated silicons. The reason why the edge-sharing tetrahedra structure originally designed was instable is also apparent. Indeed, there is an oxygen located just below the
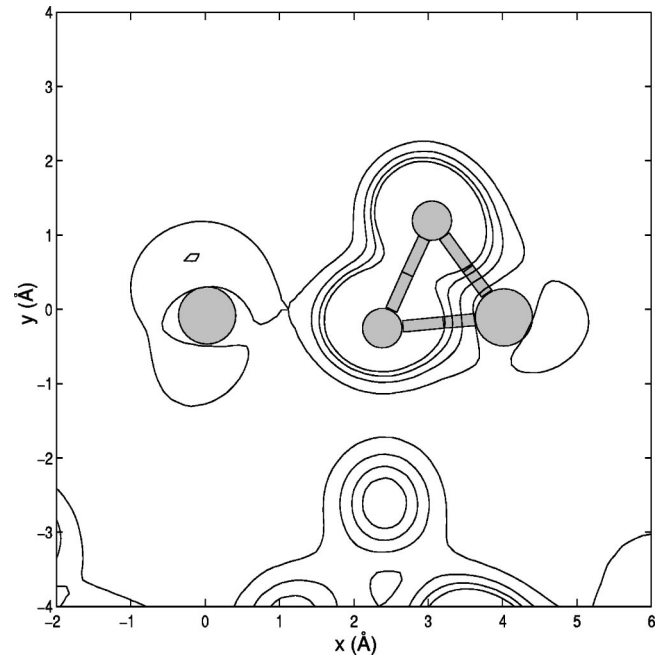

FIG. 2. Contour plot of the electronic density on the oxygen dimer at the dimer surface. The contour is drawn in a plane passing through the Si atom with the dimer, the two-coordinated Si, and the lower oxygen of the dimer. Note that the upper oxygen is almost coplanar with these atoms. The x axis is defined by the two silicons. The origin of the x and y axis (defined by orthogonality with x) is the two-coordinated Si. As a guide for the eye to locate the atoms, we superimposed (in pale gray) to the contour plot a ball and stick representation of the structure: the big circles are Si atoms while the small ones are O atoms. The oxygen dimer clearly appears at the center of the picture, while the electronic density is increased on the two-coordinated silicon with respect to four-coordinated silicons. At the bottom of the figure, there is another peak of density. It corresponds to an oxygen located just above the dimer which repels it towards the outside. The contour interval is 0.5 e$^-$/Å^3.
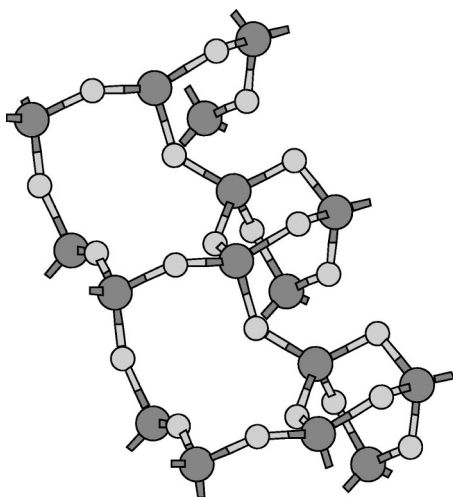
FIG. 3. Top view of the semidense surface. Si and O atoms are represented in dark and pale gray, respectively.

dimer (at the bottom of the figure) which repels it towards the outside.

B. The semidense surface

By slightly displacing this oxygen in order to avoid the steric effect, and allowing for more atomic relaxation, we obtain a new 2×1 reconstruction. This third surface model presents chains of three-membered rings (Fig. 3) which produce a densification of the outermost O-Si-O layer. In this structure, which we refer to as the *semidense* surface, all the Si and O atoms are four-fold coordinated and two-fold coordinated, respectively. This is consistent with the higher stability of the semidense surface compared to the cleaved surface (see Table I).

C. The VAP surface

By heating the dimer surface up to 300 K, we obtained our fourth model, which is also a 2×1 reconstruction. It is more stable than the cleaved surface, though less stable than the semidense surface (see Table I). In this structure, all the Si atoms are four-coordinated but there is a one-coordinated oxygen and a three-coordinated oxygen per surface unit cell. (A side view of this structure is reported in Fig. 4). The two
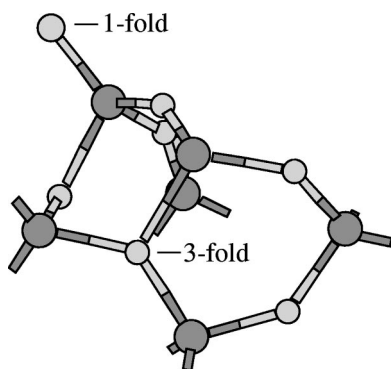

FIG. 4. Side view of the VAP surface. Si and O atoms are represented in dark and pale gray, respectively. The one-coordinated and three-coordinated oxygens are indicated. Note also the presence of three-membered rings.
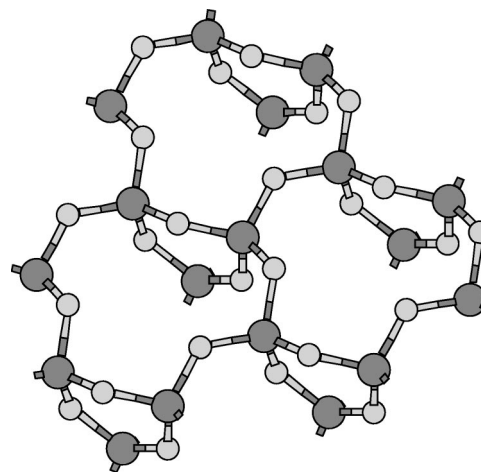

FIG. 5. Top view of the dense surface. Si and O atoms are represented in dark and pale gray, respectively.

oxygen atoms are bonded to two different Si atoms, with the one-fold coordinated O pointing towards the outside. This surface is also characterized by the presence of three-membered rings, with the three-fold coordinated O being attached to one of these rings. Such an association of a three-fold O with a three-membered ring has also been observed in classical simulations of amorphous silica surfaces.[8] The increased stability with respect to the dimer surface can be attributed to the creation of the same number of Si-O bonds as in an idealized fully coordinated network (see Table I).

The pair of over- and undercoordinated O atoms may be referred to as a valence alternation pair. The VAP concept was first introduced by Kastner[26] in his study of chalcogenide glasses (e.g., As_2Se_3). A valence alternation pair was formed when two chalcogen atoms, both twofold coordinated in the ground state, rearranged instead into one positively charged three-coordinated atom and one negatively charged one-coordinated atom. It was proposed that the density of VAP's in most glasses is relatively large since the creation of such a defect requires a relatively small energy. Their existence in amorphous SiO_2 was first proposed by Lucovsky[27] based on the interpretation of infrared and Raman spectra. This author estimated the density of these defect pairs to be quite large, of the order of 10^{19} cm^{-3}.[28,29]

D. The dense surface

The most stable reconstruction is obtained by heating the cleaved surface up to 300 K. During the molecular-dynamics simulation, the uppermost O-Si-O layer merges with the second layer with the formation of three-membered and six-membered rings (Fig. 5) that do not exist in bulk α-quartz. This reconstruction presents only four-coordinated Si and two-coordinated O with no dangling bonds. The outermost O-Si-O layer is denser than those located in the bulk, due to the merging of two layers of the original structure (Fig. 6). As in the cleaved surface case, the first atomic plane of the surface contains O atoms only, but this plane contains now three times more atoms. Indeed, the two planes of oxygens from the outermost layer in the cleaved surface [O(1U) and O(1D) in Fig. 6] have merged with the upper plane of oxygens of the second O-Si-O layer [O(2U)]. The first plane of

O(1U)
Si(1)
O(1D)
O(2U)　　　　　　　　O(1U+1D+2U)
Si(2)　　　　　　　　Si(1+2)
O(2D)　　　　　　　　O(2D)
O(3U)　　　　　　　　O(3U)
Si(3)　　　　　　　　Si(3)
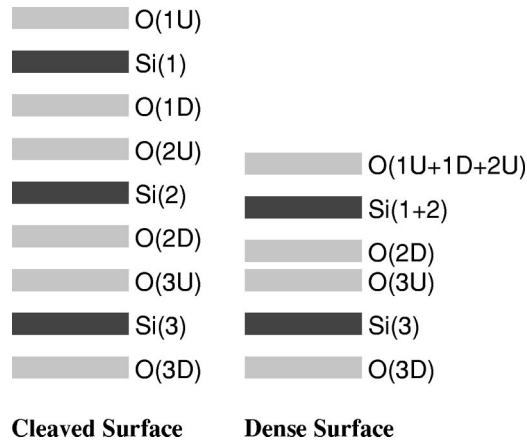O(3D)　　　　　　　　O(3D)

Cleaved Surface　　　　**Dense Surface**

FIG. 6. Schematic view of the reconstruction of the cleaved surface (left side of the graph) into the dense surface (right side of the graph). The planes of Si and O atoms are represented in dark and pale gray, respectively. For the cleaved surface, three O-Si-O layers have been represented and labeled from 1 to 3 starting from the surface. In each layer, the upper and lower planes of oxygens have been distinguished: U(up) and D(down), respectively. For the dense surface, the same number of atoms has been represented. However, due to the densification, there are only two O-Si-O layers left. In each plane, we have indicated the origin of the atoms by their label. For instance, the upper O layer corresponds to the merging of the O(1U), O(1D), and O(2D) planes.

Si atoms is also denser, containing twice the number of atoms [Si(1+2)] than in the cleaved surface. The lower plane of oxygens of the second O-Si-O layer has almost merged with the upper plane of oxygens of the third O-Si-O layer. The atomic arrangement in deeper layers is almost unaffected by these changes, and the bulk crystal structure is recovered rapidly.

By computing the total energy for a set of intermediate configurations derived from the constant-temperature MD run, the energy barrier separating the cleaved from the dense surface was estimated to be roughly 0.02 eV/Å^2. The saddle point corresponds to a structure very similar to the VAP surface with a one-fold coordinated oxygen and a three-fold coordinated oxygen per surface unit cell (however, since we have a 1×1 geometry, the concentration of those defects is twice here than in the VAP surface).

E. Relative stability and electronic properties

The stability of the VAP, the semidense, and the dense surfaces was tested by heating these surfaces up to 3500 K for 300–400 fs (depending on the system).[30] No further reconstruction was observed indicating a relative stability of these surface structures, though other possible reconstructions cannot be excluded.[31] In order to obtain the absolute surface energies for the various models, we compute the total energy of slabs containing 10 and 12 monolayers of SiO_2, respectively, which present the cleaved surface model on both ends. By comparison with the total energy of an equivalent amount of bulk α-quartz, we find that the surface energy for the cleaved surface is 0.17 eV/Å^2 (this value changes by less than 1% when the number of monolayers increases from 10 to 12). The absolute surface energies for the various models have been reported in Table I.
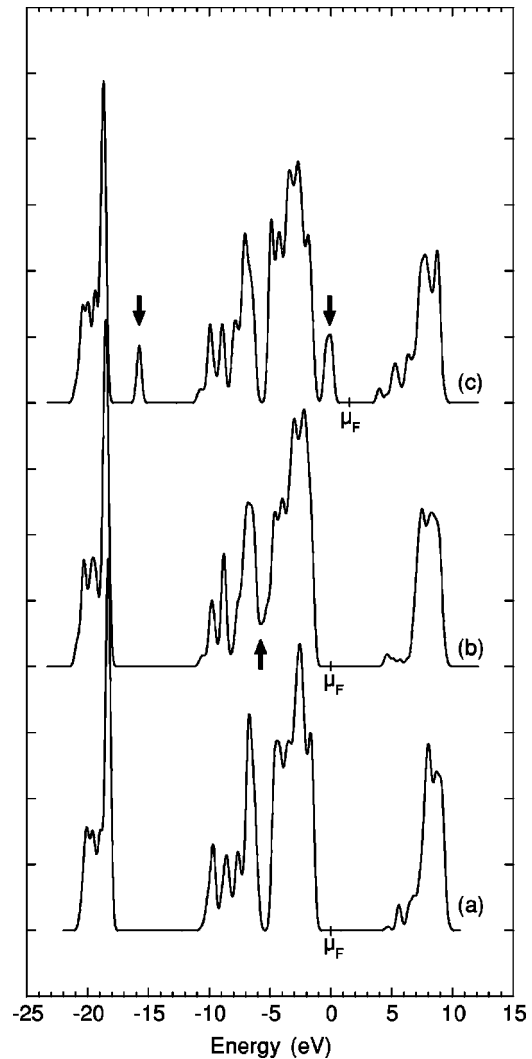

FIG. 7. Electronic density of states for (a) bulk α quartz, (b) the dense surface, and (c) the cleaved surface. The fermi level for the bulk α-quartz and for the dense surface are aligned ($\mu_F = 0$ eV), that of the cleaved surface has been shifted $\mu_F = 1.5$ eV, in order to facilitate the comparison between the different parts.

Finally, we have computed the electronic density of states (DOS) for the dense and the cleaved surface, by using the ABINIT code.[32] The calculated DOS of the cleaved surface [part (c) in Fig. 7] is very similar to the bulk quartz one [part (a) in Fig. 7]. However, two extra peaks appear (marked by arrows), corresponding to electronic states mostly located on the nonbridging oxygen atoms. The first peak is located near the O $2s$ states, while the second one is situated in the former band gap region, so that the actual band gap is reduced. The DOS associated to the dense surface [part (b) in Fig. 7] is also similar to that of bulk quartz. The main difference (marked by an arrow) is the disappearance of the gap between the Si-O bonding and O $2p$ nonbonding states. Such a feature also appears in SiO_2 under pressure;[12,13] it indicates a strong hybridization between these states. Presumably, the lone pair on the oxygen atoms from the outermost layer are much more delocalized than in the bulk.

IV. CONCLUSIONS

We have presented an investigation of the (0001) α-quartz surface within a first-principles approach. We

started with two initial configurations, the cleaved surface (with nonbridging oxygens at the top) and an unstable 2×1 reconstruction with edge-sharing tetrahedra. We obtained two models by performing atomic relaxation of the 2×1 reconstruction. One of these is a fairly stable reconstruction, called the semidense surface, presenting three-membered rings chains. We also presented two other stable reconstructions, obtained by performing constant-temperature molecular-dynamics simulations. The first, named the valence alternation pair surface, involves the presence of paired over- and undercoordinated oxygen atoms located near the surface, and of three-membered rings. The second reconstruction, called the dense surface, topologically imitates the bulk, in that, thanks to a densification of the two uppermost layers of SiO_2 tetrahedral units with three-membered and six-membered rings, the coordination of all O and Si atoms is bulklike. By computing their respective surface energy, we found that the dense surface is the most stable of all investigated structures, and we propose this as a candidate model structure for the dry reconstructed (0001) surface obtained upon cleaving. The calculated electronic density of states for this surface is very similar to the one of bulk α-quartz, apart from the disappearance of the gap between bonding antibonding O $2p$ states.

*Present address: Department of Chemistry and Princeton Materials Institute, Princeton University, Princeton, New Jersey 08544.

[1] *The Physics and Chemistry of SiO₂ and the Si-SiO₂ Interface*, edited by C.R. Helms and B.E. Deal (Plenum Press, New York, 1988).

[2] Q. Zhong, D. Innis, K. Kjoller, and V.B. Ellings, Surf. Sci. Lett. **290**, L688 (1993).

[3] I. Janossy and M. Menyhard, Surf. Sci. **25**, 647 (1974).

[4] F. Bart and M. Gautier, Surf. Sci. Lett. **311**, L671 (1994).

[5] S. Noge *et al.*, Jpn. J. Appl. Phys., Part 1 **36**, 3081 (1997).

[6] S.H. Garofalini, J. Chem. Phys. **78**, 2069 (1983).

[7] B.P. Feuston and S.H. Garofalini, J. Chem. Phys. **89**, 5818 (1988).

[8] B.P. Feuston and S.H. Garofalini, J. Chem. Phys. **91**, 564 (1989).

[9] S.H. Garofalini, J. Non-Cryst. Solids **120**, 1 (1990).

[10] M.L. Hair, *Infrared Spectroscopy in Surface Chemistry* (Dekker, New York, 1967).

[11] R.K. Iler, *The Chemistry of Silica* (Wiley, New York, 1979).

[12] N. Binggeli, N. Troullier, J.L. Martins, and J.R. Chelikowsky, Phys. Rev. B **44**, 4771 (1991).

[13] A. Di Pomponio and A. Continenza, Phys. Rev. B **50**, 5950 (1994).

[14] R. Car and M. Parrinello, Phys. Rev. Lett. **55**, 2471 (1985).

[15] F. Tassone, F. Mauri, and R. Car, Phys. Rev. B **50**, 10 561 (1994).

[16] P. Hohenberg and W. Kohn, Phys. Rev. **136**, B864 (1964); W. Kohn and L.J. Sham, Phys. Rev. **140**, A1133 (1965).

[17] F. Liu, S.H. Garofalini, D. King-Smith, and D. Vanderbilt, Phys. Rev. B **49**, 12 528 (1994), and references therein.

[18] D.R. Hamann, Phys. Rev. Lett. **76**, 660 (1996).

[19] In order to study the hydration of the (0001)α-quartz, we have considered the various surfaces with water molecules located 5 Å away, as a starting point. And, in this case, we have used the GGA. Even though these systems are not strictly equivalent to those used in the present study, the energy differences can be compared, since in principle the water molecules do not interact with the surface.

[20] N. Troullier and J.L. Martins, Phys. Rev. B **43**, 1993 (1991).

[21] J.P. Perdew and A. Zunger, Phys. Rev. B **23**, 5048 (1981).

[22] N.R. Keskar and J.R. Chelikowsky, Phys. Rev. B **46**, 1 (1992).

[23] L. Levien, C.T. Prewitt, and D.J. Weidner, Am. Mineral. **65**, 920 (1980).

[24] S. Nosé, Prog. Theor. Phys. Suppl. **103**, 1 (1991).

[25] G.-M. Rignanese, Ph.D. thesis, Université Catholique de Louvain, 1998. A postscript file is available at the following URL: http://www.pcpm.ucl.ac.be/~rigna/docs/thesis.ps.gz

[26] M. Kastner, D. Adler, and H. Fritzsche, Phys. Rev. Lett. **37**, 1504 (1976).

[27] G. Lucovsky, Philos. Mag. B **39**, 513 (1979).

[28] G. Lucovsky, J. Non-Cryst. Solids **35&36**, 825 (1980).

[29] F. Grey and R. Feidenhans'l, Europhys. News **19**, 94 (1988).

[30] Our simulations are highly CPU-time consuming. This has prevented us from performing longer runs.

[31] In constant-temperature molecular-dynamics, the transition probability for a reconstruction to occur is proportional to $\exp(-\Delta E/k_b T)$, where ΔE is the energy barrier involved. Hence, one has to play with the temperature and the duration of the simulation in order to increase the probability to observe a reconstruction. As an example, the reconstruction of the cleaved surface into the dense surface, for which we have estimated the energy barrier to be 0.02 eV/Å^2, occurs within 100 fs at 300 K. This gives an idea of the stability that can be expected for the VAP, the semidense, and the dense surfaces, which do not reconstruct after 300–400 fs at 3500 K.

[32] The ABINIT code is a joint project of the Université Catholique de Louvain, Corning Incorporated, and other contributors (URL http://www.pcpm.ucl.ac.be/abinit). Amongst other things, it relies on an efficient fast Fourier transform algorithm (Ref. 33) for the conversion of wave functions between real and reciprocal space, on the adaptation to a fixed potential of the band-by-band conjugate gradient method, (Ref. 34) and on a potential-based conjugate-gradient algorithm for the determination of the self-consistent potential (Ref. 35).

[33] S. Goedecker, SIAM J. Comput. **1**, 1605 (1997).

[34] M.C. Payne, M.P. Teter, D.C. Allan, T.A. Arias, and J.D. Joannopoulos, Rev. Mod. Phys. **64**, 1045 (1992).

[35] X. Gonze, Phys. Rev. B **54**, 4383 (1996).